400 V/1000 kVA Hybrid Automatic Transfer Switch

Bing Tian, Chengxiong Mao, *Senior Member, IEEE*, Jiming Lu,
Dan Wang, *Member, IEEE*, Yu He, Yuping Duan, and Jun Qiu

***Abstract*—A lot of large-scale industrial critical loads suffer from voltage interruptions and sags which can cause a significant financial loss. The thyristor-based solid-state transfer switch (STS) and mechanical-based automatic transfer switch (ATS) are used to protect loads against these power quality problems. However, the STS has a great deal of loss consumption because of the forward voltage drop of the thyristors, and ATS can hardly satisfy the voltage-sensitive load due to the long transfer time. This paper proposes a 400 V/1000 kVA hybrid ATS (thyristor switch in parallel with mechanical switch) (HATS) to realize low power consumption under normal situation and transfer fast when required. The proposed HATS has four transfer strategies which can be chosen according to different applications, it realizes the overlapping transfer of the neutral wire, and it can make a decision to transfer or not according to the different fault locations (transfer on the source side and not transfer on the load side). The design details of the prototype are presented, and laboratory tests and field experiments show the prototype good performance.**

***Index Terms*—Hybrid transfer switch, power quality, power supply reliability, transfer switch.**

I. Introduction

POWER quality problems have been always troubling the large-scale industries, such as the iron and steel industry. Voltage interruptions and sags will lead to pool quality products or make the production line paralysis in severe cases. These accidents may cost significant financial loss to industrial customers [1]–[4]. The uninterruptible power supply and dynamic voltage restorer are developed to overcome these problems [5]–[9], but they may not be suitable for large-scale industries due to the high cost. Generally, there are two or more power feeders in the enterprises, one as the preferred source and another as the alternate source. The thyristor-based solid-state transfer switch (STS) and mechanical-based automatic transfer switch (ATS) may be the most cost-effective solutions to the power quality problems. [10]–[17]. The transfer time of the STS is very short, and the transfer process has a smaller impact to critical loads [18]–[20]. However, STS has obvious power dissipation when thyristors are in conduction state. Therefore, STS needs a huge and expensive cooling system [21], [22].

Manuscript received May 21, 2012; revised November 2, 2012; accepted December 20, 2012. Date of publication January 9, 2013; date of current version June 21, 2013. This work was supported in part by the National Basic Research Program of China under Grant 2009CB219702 and in part by the Key Project of the National Natural Science Foundation of China under Grant 50837003. *(Corresponding author: D. Wang.)*

B. Tian, C. Mao, and Y. He are with the State Key Laboratory of Advanced Electromagnetic Engineering and Technology, Huazhong University of Science and Technology, Wuhan 430074, China (e-mail: tianbing@hust.edu.cn; cxmao@mail.hust.edu.cn; wuhanheyu2@smail.hust.edu.cn).

J. Lu and D. Wang are with the College of Electrical and Electronic Engineering, Huazhong University of Science and Technology, Wuhan 430074, China (e-mail: lujiming@mail.hust.edu.cn; wangdan@mail.hust.edu.cn).

Y. Duan and J. Qiu are with the Wuhan Iron and Steel (Group) Corporation, Wuhan 430083, China (e-mail: duanyp@wisco.com.cn; qiujun88552@sina.com).

Digital Object Identifier 10.1109/TIE.2013.2238872

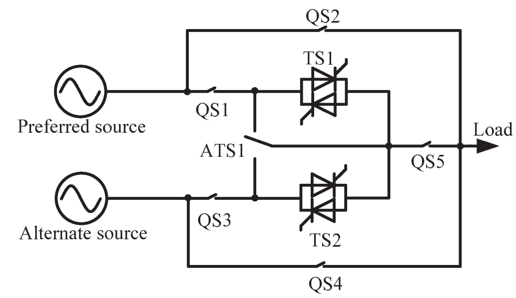

Fig. 1. Main circuit structure of HATS.

Hybrid ATS (HATS) has been proposed to reduce the loss consumption [21], [22]. The hybrid switch device proposed in [22] consists of a pair of antiparallel thyristors and a special designed mechanical parallel switch, which can open the circuit within 1 ms. However, the structure and the driving system are complicated. The HATS that this paper proposed takes the widely used ATS as the thyristors' parallel switch. The structure and driving circuit are simplified, according to the structure, and four transfer strategies are proposed to adapt to different applications. Also, the proposed HATS realizes the overlapping transfer of the neutral wire, and it can identify the fault location and make a correct decision to transfer or not.

First, operation principles, including operation rule, transfer strategy, voltage sag detection method, fault location identification method, and the overlapping transfer of the neutral wire, are discussed. Then, design details, including both hardware and software, are presented, and then, laboratory tests are carried out to verify the principles. Finally, field experiments are carried out, and the results show that the prototype is functional.

II. Operation Principles

The structure of the HATS is shown in Fig. 1. TS1 and TS2 are the antiparallel thyristor switches connected to the preferred source and alternate source, respectively. ATS1 is a mechanical switch, and it has three contacts; two static contacts are connected to the preferred source and alternate, respectively, and the moving contact is connected to the load. QS1, QS3, and QS5 are isolating switches. QS2 and QS4 are bypass switches.

In order to ensure maximum reliability of power supply to load, HATS should follow the following operation rules.

1) In the normal state, only one of the two sources can be connected to the load.
2) Only when the alternate source voltage is within the normal range and has the same phase order with the preferred source does it allow transfer operation.

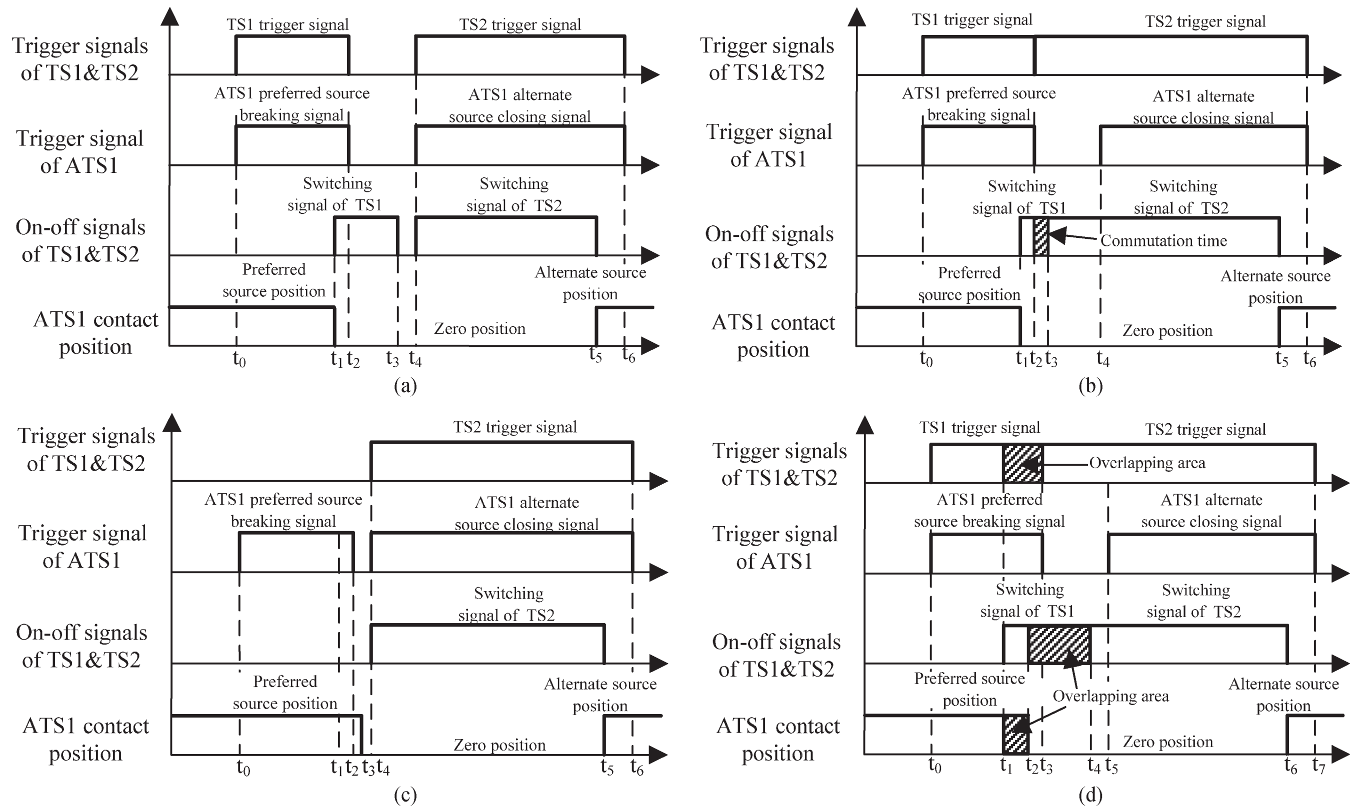

Fig. 2. Timing diagram of four transfer strategies. (a) BBM. (b) Natural commutation. (c) Mechanical switch breaking the circuit. (d) MBB.

3) During the transfer process, the device should be able to reliably connect the load to the alternate source after the preferred source has been cut off. If an unexpected error happened and the alternate source cannot be closed anyway, the device should be able to reconnect the load to the preferred source.
4) HATS should inhibit a transfer when faults happened on the load side because the transfer operation will expand the fault range.
5) Transfer should also be forbidden during overload. For example, the motor starts, and the load bus voltage may be pulled low. In this case, the transfer operation is prohibited because the load voltage will not recover even if the HATS transferred to the alternate source.

A. Transfer Strategy

Four transfer strategies suitable for HATS have been proposed for different applications according to the transfer process:

1) break before make (BBM);
2) natural commutation;
3) mechanical switch breaking the circuit;
4) make before break (MBB).

1) BBM: The structure of HATS is shown in Fig. 1, and the timing diagram of the BBM strategy is shown in Fig. 2(a); when a transfer operation is required, the controller sends the ATS1's preferred source breaking signal and TS1's gating signal at t_0. ATS1 receives the breaking signal, the moving contact begins to separate at t_1, and the current is commutated to TS1 immediately. The time $(t_1 - t_0)$ is the inherent breaking time of ATS1. TS1's gating signal is removed at t_2 (after t_1), and the current is blocked by TS1 at the first current zero-crossing point. At the time t_3, all three phases have been cut off. The controller detects the off signal and sends the ATS1's alternate source closing signal and TS2's gating signal at t_4, TS2 turns on immediately, and ATS1 takes a long time $(t_5 - t_4)$ to close to the alternate source. At the time t_6, the controller removes all gating signals, and the load is connected to the alternate source by ATS1.

During the transfer process, the load current had been cut off by thyristor switch TS1, so there is no arc between ATS1's contacts; this is very helpful for extending the contact's life. Moreover, two sources have no chance to be in parallel, so it has a good safety to feeders. This strategy is suitable for the loads which can endure a long transfer time (about 30–40 ms), and the two power sources cannot be in parallel directly.

2) Natural Commutation: Fig. 2(b) shows the process of the natural commutation strategy. Until the time t_2, the transfer process goes the same with the BBM strategy. At the time t_2, if the commutation condition (discussed later) is satisfied or it is the current zero-crossing point, the controller will trigger TS2 immediately. The time from t_2 to t_3 is the commutation time, and it is determined by commutation circuit characteristics. After the commutation, the transfer process is carried out the same with the BBM strategy.

Assume that the direction of instantaneous load current is from the preferred source to the load at t_2 [shown in Fig. 3(a)]. If the current through the TS1 decreases when TS2 is triggered on and the voltage $(u_a - u_p)$ zero-crossing point comes after the current zero-crossing point, commutation will succeed. The equivalent circuit is shown in Fig. 3(b), where u_p is the

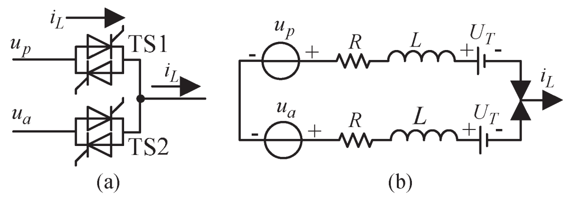

Fig. 3. Commutation circuit and the equivalent circuit. (a) Commutation circuit. (b) Equivalent circuit.

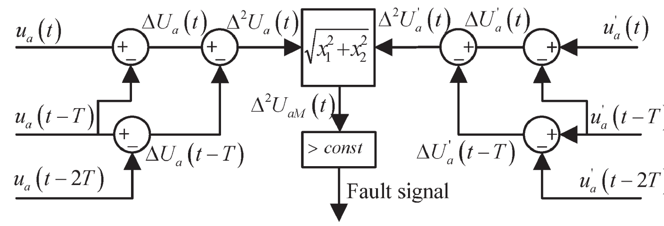

Fig. 4. Voltage sag detection diagram.

preferred source voltage, u_a is the alternate source voltage, i_L is the load current, and they are all instantaneous values. R and L are the line impedances in the commutation circuit, and U_T is the forward voltage drop of the thyristor. According to Fig. 3(b), the commutation condition is expressed as inequality (1)

$$(u_a - u_p) \times i_L > 0. \tag{1}$$

In most cases, three phases can hardly satisfy the inequality (1) at the same time, so the commutation process goes per phase, which means that there is a short time that one phase of the load is connected to the preferred source and another phase is connected to the alternate source. The controller always triggers the thyristor in TS2 which has the common cathode with the conducting thyristor in TS1. If the commutation condition cannot be satisfied anyway, TS2 will conduct current just after the load current is blocked by TS1. Because the thyristors are forced to turn off, the transfer time is shorter than that of the BBM strategy. In the power system, single-phase disturbance is the most often faults, and this strategy has little impact to undisturbed phases. Therefore, it is suitable for the three-phase load composed by three independent single-phase loads.

3) Mechanical Switch Breaking the Circuit: Mechanical switch breaking the circuit means that the load current is cut off by mechanical switch ATS1; the timing diagram is shown in Fig. 2(c). When an opening operation is required, thyristor switch TS1 is not turned on, and the load current is cut off by mechanical switch ATS1, so it is required that the ATS1 has the arc extinguishing ability. After the arc extinguished, the alternate source will be connected to the load by TS2 and ATS1 as the BBM strategy described. The time $(t_3 - t_1)$ is the arcing time, and it is usually shorter than the thyristor's freewheeling time, so this strategy has a higher transfer speed. This strategy's transfer time is mostly decided by the mechanical switch's inherent opening time, and if using a faster switch, the transfer time can be shortened, but the cost may increase greatly, so it is suitable for the sensitive load which has strict demand to transfer time and the two sources cannot be in parallel directly.

4) MBB: MBB is also known as parallel transfer or hot transfer. The timing diagram is shown in Fig. 2(d). In this strategy, TS2's gating signal is sent (at t_1) before TS1's gating signal is removed (at t_3). Before ATS1's contact begins to separate (at t_2), ATS1 and TS2 are in conduction state. Then, TS1 conducts the current until the first current zero-crossing point (t_4) or is forced to be turned off by the alternate source voltage after the gating signal had been removed at t_3. During the time $t_2 \sim t_4$, TS1 and TS2 are in conduction state. Therefore, the total paralleling time of two sources is from t_1 to t_4. This strategy has gained wide acceptance because the transient on the load bus is eliminated, assuming that the two sources are in phase. However, the cross-current, determined by the voltage difference between the two sources, may be very high and exceed the short-term withstand ratings of the transformers and switches, so this transfer strategy demands that two sources are in phase. The MBB strategy satisfies the seamless transfer demand of the loads.

B. Voltage Sag Detection

Voltage sag detection is very important to HATS. This paper proposes a rapid and reliable detection method shown in Fig. 4. The basic principle of this method is to detect the voltage difference between the current value and the value a cycle before and, at the same time, detect the difference between the current derivative value and the derivative a cycle before. Therefore, there is no dead area of the detection. In actual use, the derivative is replaced by the difference, and there is sufficient accuracy when the sampling time is 1/24 cycle.

Assume that the voltage satisfied

$$u_a(t) = U_m \sin(\omega t + \phi). \tag{2}$$

Define

$$u_a'(t) = \frac{1}{\omega}\left(\frac{d}{dt}u_a(t)\right) = U_m \cos(\omega t + \phi) \tag{3}$$

where $\omega = 2\pi \cdot f$ is considered as a constant. If the voltage sag occurs at time t_k and the amplitude falls $a (0 < a < 1)$, the points between t_k and $(t_k + T)$ are shown as

$$u_a(t) = (1-a)U_m \sin(\omega t + \phi),\ t_k < t < (t_k + T) \tag{4}$$

$$u_a'(t) = (1-a)U_m \cos(\omega t + \phi),\ t_k < t < (t_k + T). \tag{5}$$

Therefore,

$$\begin{aligned}\Delta U_{aM}^2(t) &= \sqrt{(\Delta U_a^2(t))^2 - (\Delta U_a'^2(t))^2} \\ &= aU_m,\ t_k < t < (t_k + T).\end{aligned} \tag{6}$$

$\Delta U_{aM}^2(t)$ is considered as the observed variable to reduce the noise and the quantization error. From (6), $\Delta U_{aM}^2(t)$ represents the extent of the voltage sag. The constant compared to $\Delta U_{aM}^2(t)$ can be set by the user through the human–machine interface. One time detection may make a mistake. According to the experience, three or more successive detections can make an accurate judgment. In actual use, to avoid detection failure under the situation that voltage decreases in a slow fashion, the fast Fourier transform method works with this rapid detection method.

C. Fault Location Identification

Fault location identification is also important because HATS has to make a decision to transfer or not according to the different fault locations. If the fault happens on the source side, the transfer operation is required immediately, and on the other hand, if the fault happens on the load side, the transfer operation should be forbidden. According to different load types, different phenomena will be observed to identify the fault location.

1) RL Load: After the fault happens, the RL load will not inject current to the fault point. When the fault location is on the source side, the current HATS detected decreases; when the fault location is on the load side, the current HATS detected increases. Therefore, HATS can identify the fault location according to the variation of the detected load current.

2) Regenerative Load: Under regenerative load conditions, the regenerated voltage will inject current to the fault point, and HATS will detect the current over the normal lever whether the fault happened on the source side or on the load side. This increases the difficulty of the fault location identification. Fortunately, the direction of the power is opposite when the fault location is different, and the power is positive when the fault is on the load side and negative when the fault is on the source side, so power direction can be used to identify the fault location. However, unfortunately, the voltage is pulled low and close to zero in serious cases such as the three-phase short-circuit fault, so the fault voltage can hardly be used directly to calculate the power. In order to get the power, a virtual phase-locked loop (PLL) voltage, in phase with the normal source voltage, without disturbance, is generated to use in the calculation.

D. Overlapping Transfer of Neutral Wire

In the T-NC distribution system, the neutral wire is usually reliably grounded near the distribution transformer, and it cannot be cut off because it is also the ground protection line. The thyristor in series with the neutral wire is not allowed because its semiconductor characteristic may lead to the unreliable grounding of the neutral wire. Conventional STS usually does not transfer the neutral wire, but it may not be suitable when the system contains a single-phase load. A four-pole mechanical transfer switch can easily transfer the neutral wire, but the neutral pole usually transfers synchronously with the phase poles, so the neutral wire is cut off, and the equipment on the load side loses the protective grounding during the transfer. This is a threat to the safety of the equipment and the operator. In order to ensure the reliable grounding of the equipment on the load side, the overlapping transfer of the neutral wire is necessary. It means that there is a little time that the load's neutral wire should be connected to both the preferred source and alternate source.

The HATS has an independent small-capacity mechanical transfer switch (ATS2 in Fig. 5) to deal with the neutral wire. During the transfer process, the controller ensures that the four-pole mechanical switch (ATS1 in Fig. 5) completes its transfer and then starts the transfer of the ATS2. As the Fig. 5 shows, ATS2 is in parallel with the neutral pole of the ATS1, and when the ATS1 breaks, the preferred source, at the mean while, breaks the neutral wire between the preferred source and the load, but ATS2 is still connecting the load neutral wire to the preferred source. Then, ATS1 connects the load to the alternate source, and until this time, ATS2 did not transfer, so the load's neutral wire is connected to both the preferred source, and the alternate source after the controller confirms that the ATS1 is connected to the alternate source; then, ATS2 starts the transfer, and after ATS2 completes its transfer, both the ATS1 and ATS2 are connected to the alternate source.

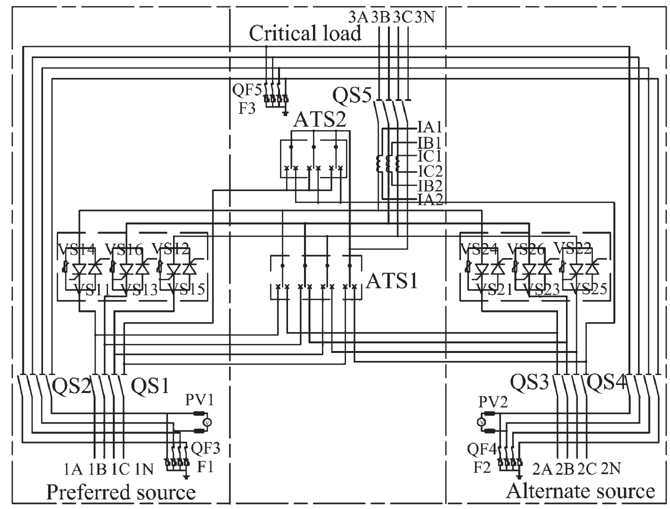

Fig. 5. Main circuit of the HATS.

III. Industrial Prototype Design

A. Main Circuit

Fig. 5 shows the main circuit of the prototype, which mainly consists of a three-phase thyristor-based switch (VS11–VS16) connecting the preferred source to the sensitive load, another three-phase thyristor-based switch (VS21–VS26) connecting the alternate source to the sensitive load, a four-pole mechanical switch (ATS1) in parallel with the thyristor switches, and a small-capacity mechanical switch (ATS2) in parallel with the fourth pole of the ATS1. Q1, Q3, and Q5 are mechanical isolating switches; Q2 and Q4 are mechanical bypass switches. These switches are used for maintenance.

The thyristors and the mechanical switches are chosen by rated voltage and rated current. The HATS is designed for 400-V line voltage applications, so the rated phase voltage $U_\Phi = 400/\sqrt{3} = 230.9$ V. The thyristor's rated voltage should be two to three times the peak of the phase voltage for safety consideration, and also considering that the load may be capacitive, the voltage on the thyristors may double. Therefore, the range of the thyristor's rated voltage is decided by the inequality (7)

$$2 \times U_\Phi \times \sqrt{2} \times 2 \leq U_R \leq 3 \times U_\Phi \times \sqrt{2} \times 2$$
$$\Rightarrow 1306.4 \text{ V} \leq U_R \leq 1959.6 \text{ V}. \tag{7}$$

The designed capacity is 1000 kVA, so the phase current $I_\Phi = S/\sqrt{3}V_l = 1000 \times 10^3/(\sqrt{3} \times 400) = 1443.4$ A, and according to the definition of the thyristor's rated current,

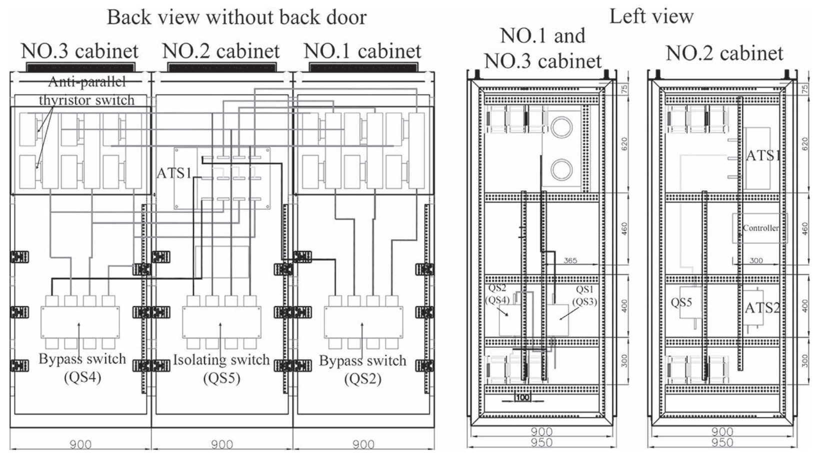

Fig. 6. Back view and left view of the HATS (units: millimeter).

the relationship between the RMS current I flow through the thyristor and the rated current I_R is defined by

$$I = 1/2\pi I_R = 1.57 I_R. \tag{8}$$

Usually, taking 1.5 to 2 times the phase current to calculate the thyristor's rated current and considering the fault current (three to seven times the I_Φ, considered to be five times in this design) flow from the regenerative load to the fault point when the fault happens on the source side, the current $I = 1/2 I_\Phi$, so the thyristor's rated current is decided by the inequality (9)

$$\begin{aligned} &1.5 \times 5 \times I_\Phi/2 \leq 1.57 I_R \leq 2 \times 5 \times I_\Phi/2 \\ &\Rightarrow 3447.5\ \text{A} \leq I_R \leq 4596.7\ \text{A}. \end{aligned} \tag{9}$$

According to the inequalities (7) and (9), the thyristor 5STP45Q2800 produced by ABB can satisfy the design needs. The rated voltage is 2800 V, and the rated current is 5490 A. An aluminum radiator is used to fix the thyristors, and nature cooling can satisfy the cooling requirements.

The mechanical parallel switch ATS1 is required to have a high opening speed. The four-pole three-position switch TBBQ-3-16/4P-III produced by TAIYONG Corporation is suitable for the ATS1. The rated current is 1600 A, and the short-time withstand current is 32 kA. The inherent opening time is in the range of 17–20 ms, and the closing time is in the range of 110–140 ms according to the test. A single-pole transfer switch is suitable for the ATS2 in principle, but the three-pole transfer switch is more common in the market. Therefore, the three-pole transfer switch TBBQ3-04/3P-III, also produced by TAIYONG, is chosen as the ATS2. In actual use, the three poles are tied together as one pole. The rated current is 400 A, so three poles in parallel are 1200 A, and it can satisfy the needs of the neutral wire.

All parts of the prototype are put into three cabinets, including a preferred source cabinet (NO.1), an alternate source cabinet (NO.3), and an output cabinet (NO.2). Fig. 6 shows the back and the left view of the HATS. The preferred source will be connected to the input port of the QS1, the alternate source will be connected to the input port of the QS3, and the load will be connected to the output port of the QS5. The controller is located in the middle position of the output cabinet.

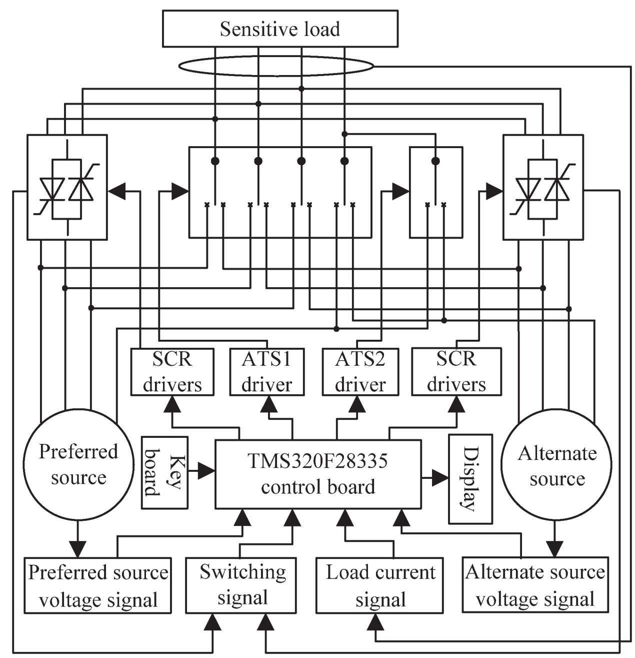

Fig. 7. Controller block diagram of the HATS.

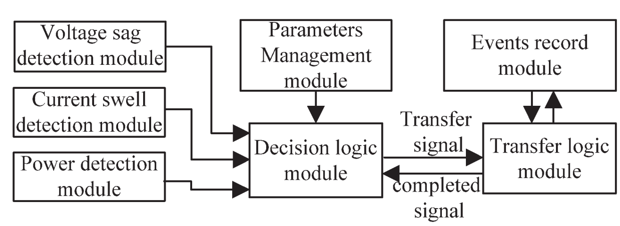

Fig. 8. Procedure modules of the HATS.

B. Control System Design

Fig. 7 depicts the controller and the periphery circuits of the HATS. The hardware system includes a dc power supply, a control board based on the DSP TMS320F28335, sample circuits of the preferred source voltage, alternate source voltage, load current and switching signal, two SCR driver units, an ATS1 driver, an ATS2 driver, a keyboard, a display unit, a communication unit, etc.

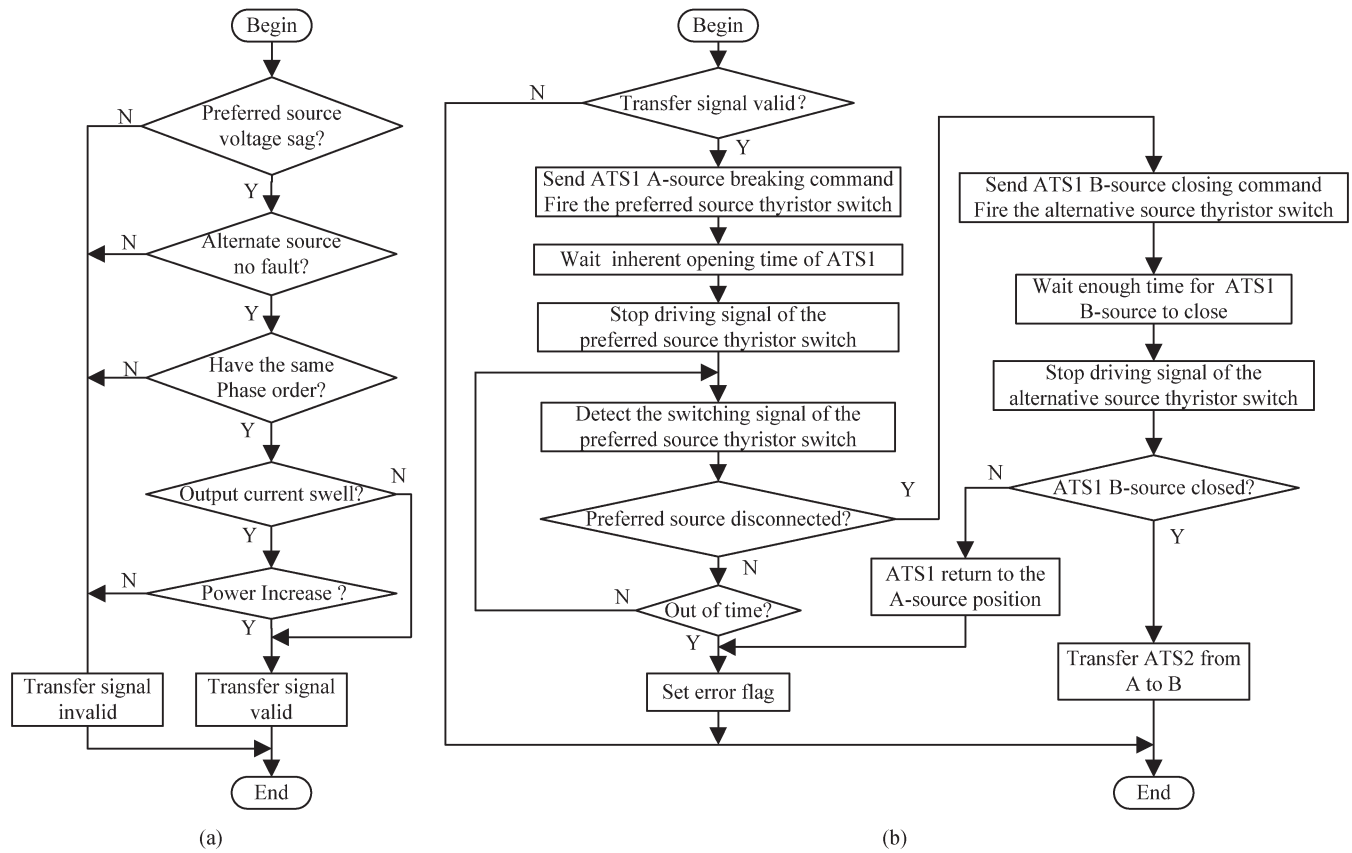

Fig. 9. Program flowchart. (a) Decision logic module. (b) Transfer logic module.

C. Procedure Design

The major procedure modules of the HATS are shown in Fig. 8, including a voltage sag detection module, a current swell detection module, a power calculation module, a parameter management module, a decision logic module, a transfer logic module, and an event record module. The decision logic module decides to transfer or not according to the parameters and signals given by corresponding modules. Then, if the transfer signal given by the decision logic module is valid, the transfer logic module will start a transfer and control the transfer process. The event record module will record the real time data during the transfer process and send the data to the host computer for further analysis. After the transfer, a completed signal will be sent to the decision logic module, and the procedure will prepare for the next transfer.

The program flowchart of the decision logic module and the transfer logic module is shown in Fig. 9. The decision logic module solves the problem of the fault location identification. Fig. 9(a) shows that the transfer signal will be valid under the following conditions.

1) There is no load current swell. This situation occurs when the load is a kind of RL load and the fault location is on the source side or the voltage sag is caused by other reasons but not the short-circuit fault near the device.
2) There is a load current swell, and at the same time, power declines quickly and reverses (flows from load to source). This situation happens when the fault location is on the source side and the load is regenerative. The regenerated voltage will lead to a reversed current. If voltage sag happens, a virtual PLL voltage will be used to calculate the power. Therefore, when the fault happens on the load side, the current flows from the source to the load, and power increases quickly; when the fault happens on the source side, the current reverses, and power decreases quickly to a negative value. According to the varying direction of the power, the fault location can be identified.

The program flowchart of the transfer logic module is shown in Fig. 9(b). ATS1 and ATS2 have three positions. A-position means that the load is connected to the preferred source, B-position means that the load is connected to the alternate source, and zero-position means that the load is connected to no source. The flowchart shows that the transfer process follows the BBM strategy. During the transfer process, if the HATS cannot transfer the load to the alternate source, it will try to return to the preferred source for the maximum power reliability. After ATS1 transfers to the alternate source reliably, ATS2 starts its transfer. This ensures that the neutral wire will not be cut off during the transfer.

D. Industrial Prototype

The HATS and the controller that this paper designed are shown in Fig. 10. It can work in the automatic mode or manual mode selected by the user through a selector on the front board

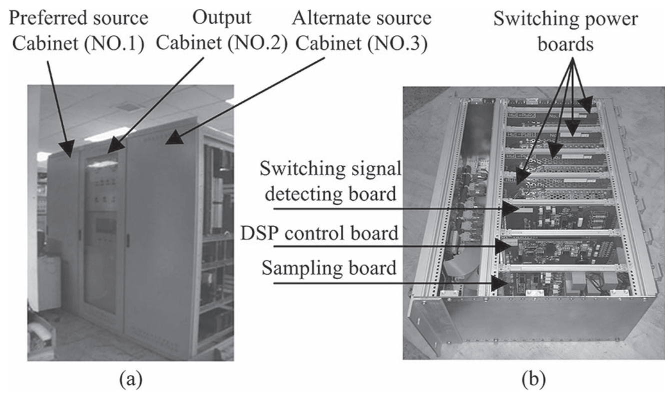

Fig. 10. Prototype and the controller. (a) Prototype. (b) Right view of the controller.

TABLE I
PARAMETERS OF THE PROTOTYPE

Rated current	1600A
Rated voltage	400V
Applications	Three phase four-wire system
Poles	4
Neutral wire	Overlapping transfer
Load type	AC-33iA
Operation mode	Auto or manual

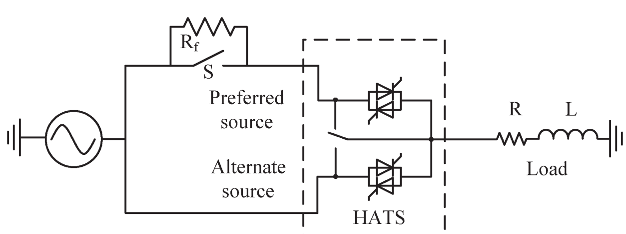

Fig. 11. Experimental wiring connection of the transfer strategies.

of the controller. In the automatic mode, the HATS will return to preferred source or not, decided by another selector when the preferred source recovers. Even when the controller runs abnormally, the HATS can still be operated manually by the three buttons below the controller on the output cabinet. The characteristics of the HATS are shown in Table I.

IV. Laboratory Tests and Results

A. Tests of the Transfer Strategies

The four transfer strategies have been implemented on the prototype and tested in the laboratory test bench. The experimental wiring connection is shown in Fig. 11, and the parameters are as follows:

1) source: 380-Vrms line voltage, three phases, and 50 Hz;
2) load: $R = 30\Omega$ and $L = 6$ mH;
3) resistance in series: $R_f = 47\ \Omega$.

R_f and a parallel switch S are used to make a voltage sag on the preferred source. The switch S is controlled manually, so the electrical angle when voltage sag happens is random.

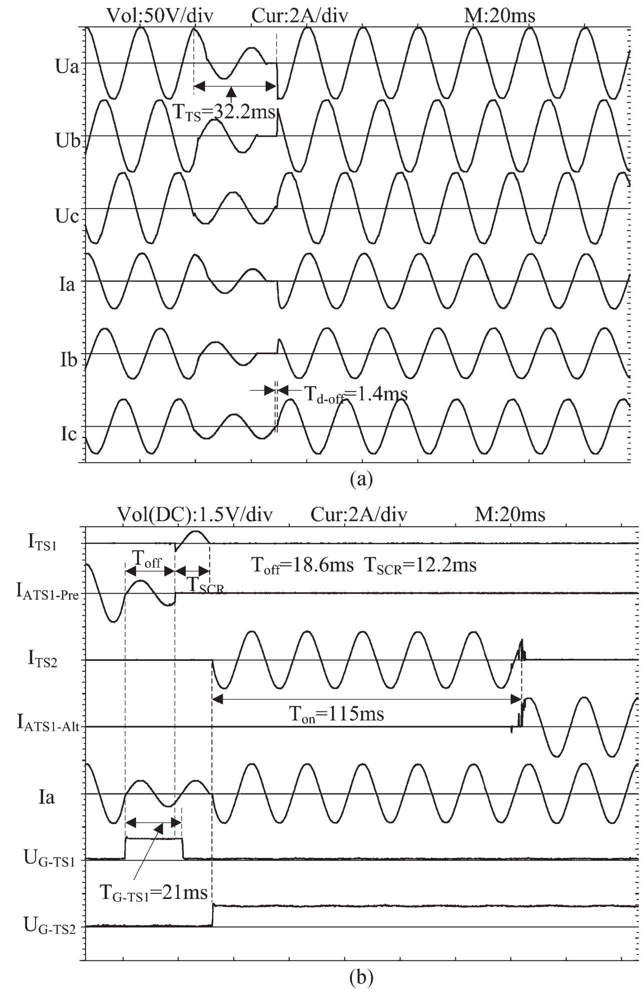

Fig. 12. Experimental waves of the BBM transfer strategy (recorded by fault recorder). (a) Load voltage and load current. From top to bottom, they are the A-, B-, and C-phase voltages and the A-, B-, and C-phase currents. (b) A-phase commutation curves. From top to bottom, they are the current of the TS1, current of the ATS1's preferred source contact, current of the TS2, current of the ATS1's alternate source contact, load current, preferred thyristor driving signal, and alternate thyristor driving signal.

1) BBM Transfer Strategy: The experimental results of the BBM transfer strategy are shown in Fig. 12. In the figure, there is a short time ($T_{\mathrm{d-off}}$, 1.4 ms) that the load is connected to no source (the time that all three-phase currents are zero). Therefore, there is no cross-current flowing between the two sources. The total transfer time (T_{TS}) is 32.2 ms. Fig. 12(b) shows the A-phase commutation curves during the transfer process. In the figure, ATS1's inherent opening time (T_{off}) is 18.6 ms, and the driving signal of the preferred source thyristor switch (TS1) should last long enough ($T_{\mathrm{G-TS1}}$, 21 ms) for ATS1's contact to separate. Therefore, when ATS1's contact begins opening, the preferred thyristor switch conducts immediately, and the thyristor's conducting time is about 12.2 ms in the figure. ATS1's inherent closing time (T_{on}) is 115 ms, and the time of the alternate thyristor driving signal should be longer than T_{on}.

2) Natural Commutation Transfer Strategy: Fig. 13 shows the experimental results of the natural commutation transfer strategy. Fig. 13(a) shows the load voltage and current waves. The commutation requirement is always satisfied according to

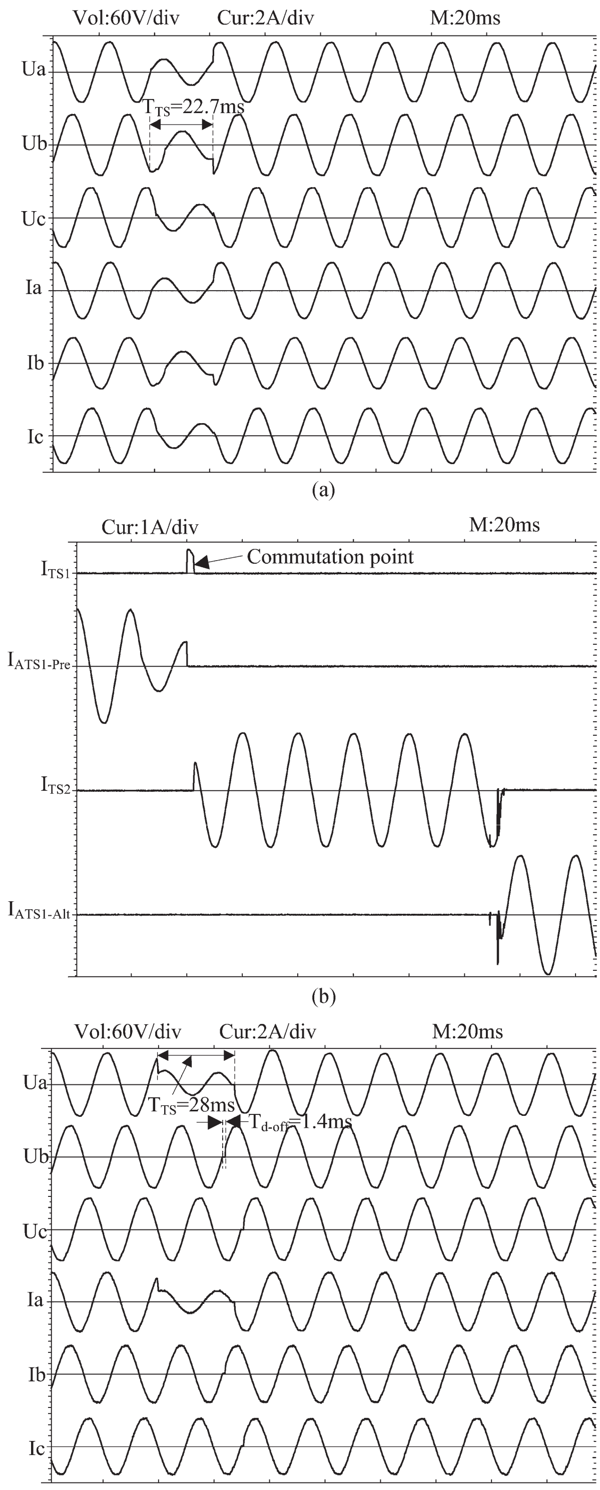

Fig. 13. Experimental waves of the natural commutation transfer strategy (recorded by fault recorder). (a) Load voltage and load current when natural commutation condition is satisfied. From top to bottom, they are the A-, B-, and C-phase voltages and the A-, B-, and C-phase currents. (b) Commutation curves of one phase. From top to bottom, they are the current of the TS1, current of the ATS1's preferred source contact, current of the TS2, and current of the ATS1's alternate source contact. (c) Load voltage and current when natural commutation condition is not satisfied.

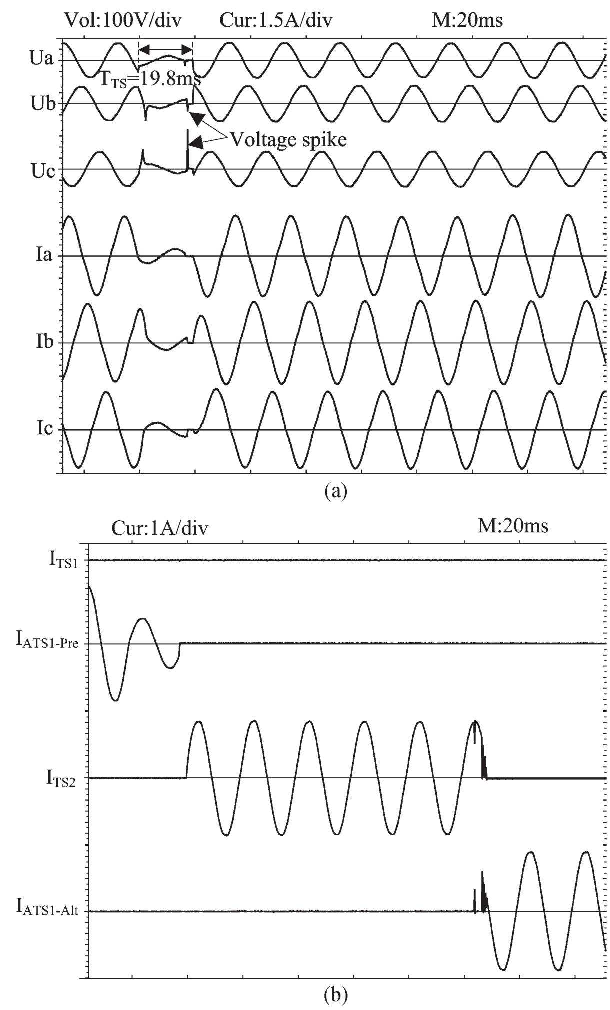

Fig. 14. Experimental waves of the transfer strategy of the mechanical switch breaking the circuit (recorded by fault recorder). (a) Load voltage and load current. From top to bottom, they are the A-, B-, and C-phase voltages and the A-, B-, and C-phase currents. (b) Commutation curves of one phase. From top to bottom, they are the current of the TS1, current of the ATS1's preferred source contact, current of the TS2, and current of the ATS1's alternate source contact.

the experimental circuit. The transfer time is about 22.7 ms, and the commutation waves of one phase are shown in Fig. 13(b). As the figure shows, the load current spends nearly no time to commutate from TS1 to TS2. In order to test how the HATS operates when the natural commutation condition is not satisfied, the judgment logic for the commutation condition is set invalid artificially in the software, and then, the test results are shown in Fig. 13(c). The transfer process goes per phase. For normal phases, the transfer is taking place at the current zero-crossing point, and the load may feel no changes during the transfer process.

3) Mechanical Switch Breaking the Circuit: Fig. 14 shows the results of the transfer strategy of the mechanical switch breaking the circuit. Fig. 14(a) shows the load voltage and current, and the transfer time is about 19.8 ms, which is mostly determined by the ATS1's inherit opening time. In the figure, there is a voltage spike when the mechanical switch ATS1 cuts off the inductive load current. Therefore, a zinc oxide nonlinear resistor is needed in parallel with the switches to protect the thyristors and the contacts. According to the transfer strategy, TS1 is not conducting current during the transfer process, and this is verified in Fig. 14(b).

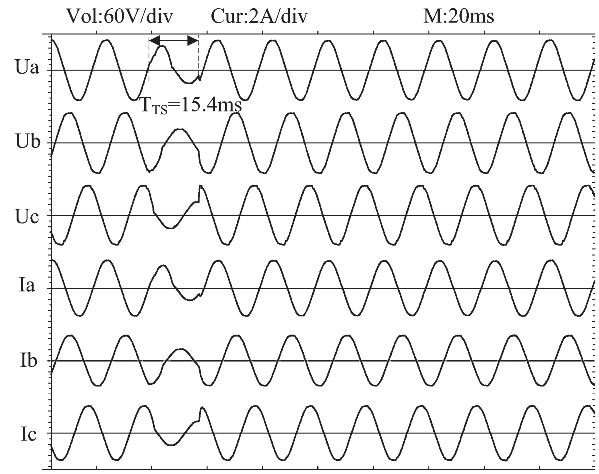

Fig. 15. Load voltage and current. From top to bottom, they are the A-, B-, and C-phase voltages and the A-, B-, and C-phase currents (recorded by fault recorder).

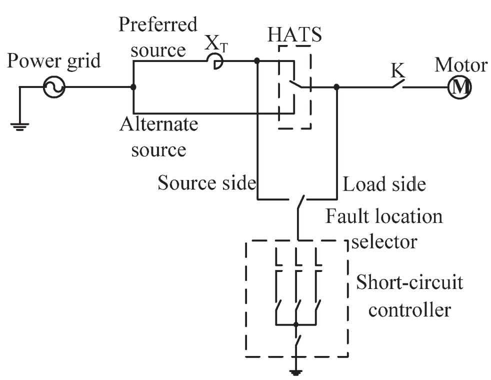

Fig. 16. Wiring connection of short-circuit experiment.

4) MBB Transfer Strategy: Fig. 15 shows the load voltage and current of the MBB transfer strategy. Since the alternate source has been connected to the load before the preferred source disconnected, the load voltage and current will not be interrupted. The transfer time in the figure is about 15.4 ms. If the controller fires the TS2 without delay when the voltage sags have been detected, the transfer time may even be shorter. However, this strategy demands that the two sources are in phase to avoid the risk of the overshoot current between them.

B. Short-Circuit Tests

Short-circuit experiments have been carried out to test the function of the fault location identification. Fig. 16 shows the experimental wiring connection. The load is a 4-kW motor, a reactor X_T is used to limit the short-circuit current, a selector is used to choose the fault location (on the source side or load side), and a short-circuit controller is used to make different types of faults. Considering the safety of the test, the BBM transfer strategy has been chosen in the short-circuit tests.

Fig. 17 shows the controller how to make a decision to transfer or not when the fault location is different. These curves are recorded by the controller itself. The preferred source voltage controller detected has no difference when the fault happens on different sides of the HATS [see Fig. 17(a) and (e)]. However, the load currents [see Fig. 17(b) and (f)] and power [see Fig. 17(c) and (g)] are extremely different. The transfer signal is valid [see Fig. 17(d)] when the fault is on the source side and invalid Fig. 17(h)] when it is on the load side. Fig. 18 shows the load voltage and load current when faults occurred on different sides. Fig. 18(a)–(d) shows the load voltage and current of the source-side faults, the HATS transferred immediately and reliably, and the time that the load voltage failed is just the transfer time. Fig. 18(e)–(h) shows the load voltage and current of the load-side faults, the HATS took no action against these faults, and the time that the load voltage failed is determined by the short-circuit controller. Four typical faults have been tested. Figs. 17 and 18 confirmed that the HATS can identify the fault location.

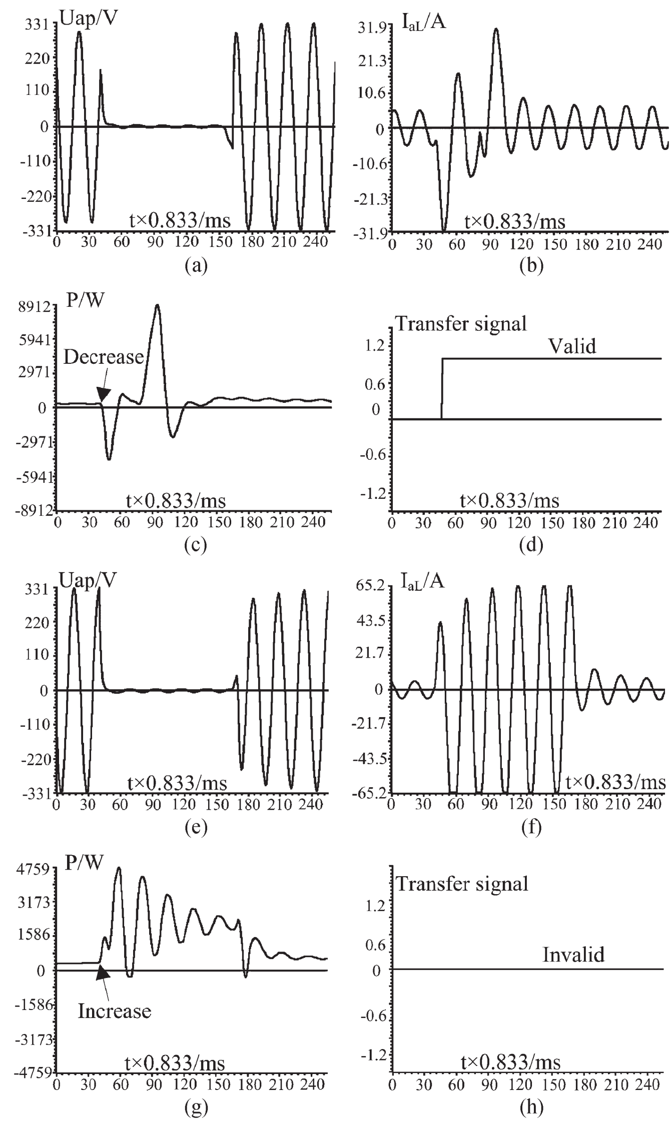

Fig. 17. Waves recorded by DSP. (a)–(d) Curves when the fault location is on the source side, and they are the preferred source A-phase voltage, load A-phase current, active power, and the transfer signal. (e)–(h) Corresponding curves when the fault location is on the load side.

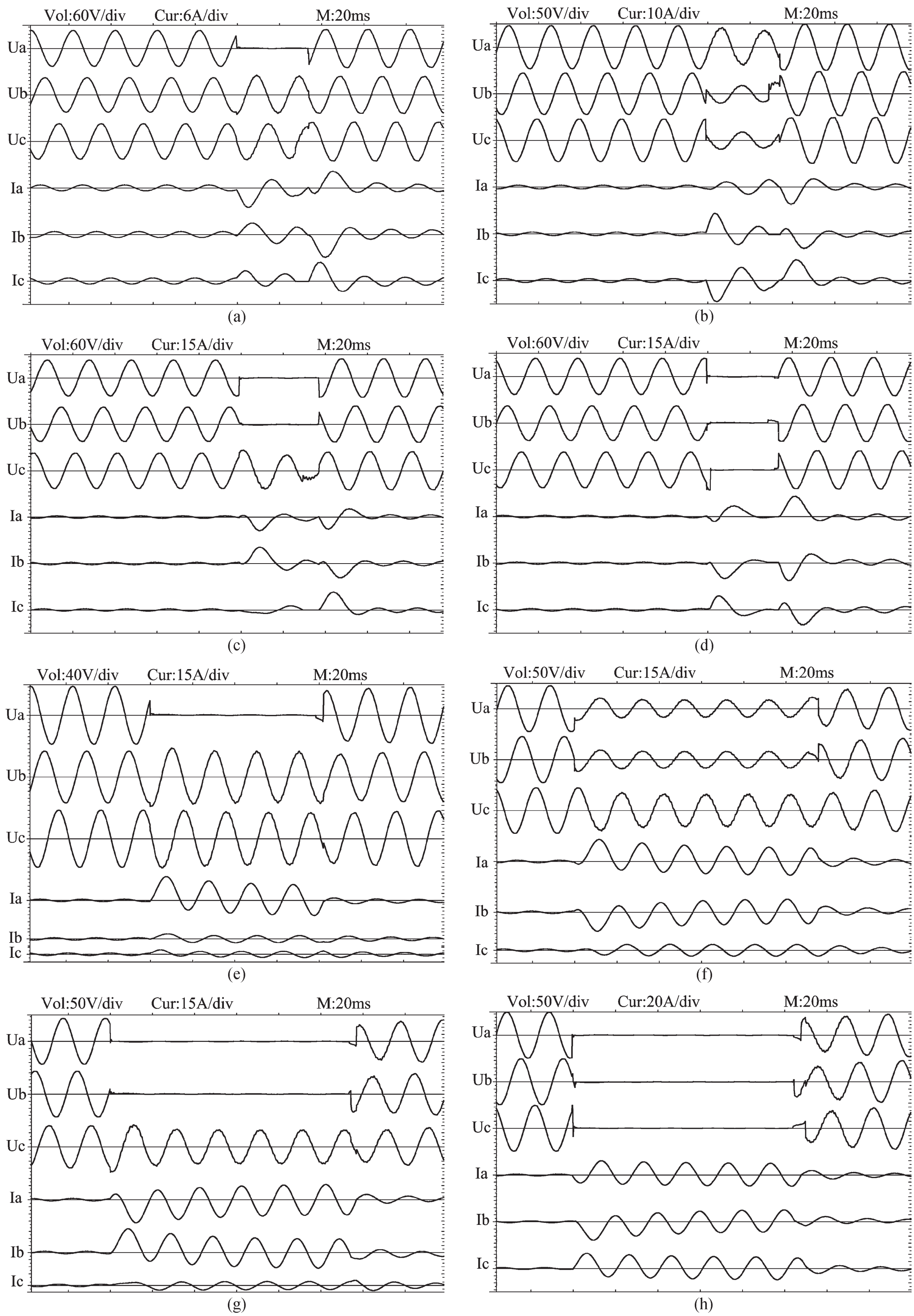

Fig. 18. Load voltage and load current waves of the short-circuit experiment (recorded by fault recorder). (a)–(d) Short-circuit experimental waves when the fault location is on the source side, and they are the phase-A grounded fault, BC-phase ungrounded fault, AB-phase grounded fault, and three-phase fault. (e)–(h) Short-circuit experimental waves when the fault location is on the load side, and they are the phase-A grounded fault, AB-phase ungrounded fault, AB-phase grounded fault, and three-phase fault.

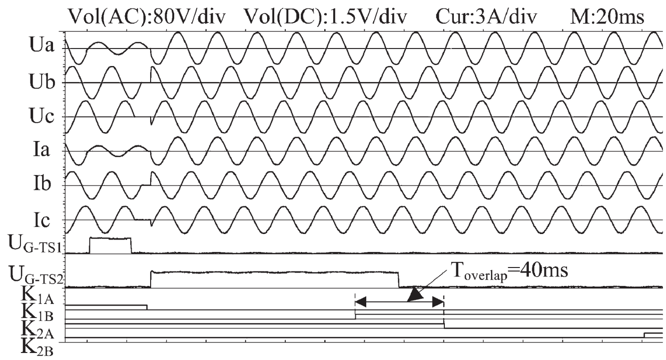

Fig. 19. Overlap transfer of the neutral wire. The previous six curves are the load voltages and currents, then followed by preferred and alternate thyristor driving signals, auxiliary contact switching signals of the ATS1's A-position and B-position, and auxiliary contact switching signals of the ATS2's A-position and B-position.

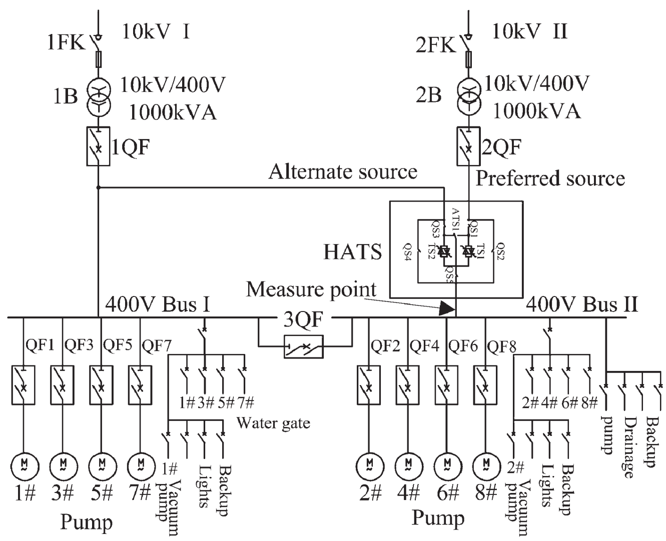

Fig. 20. Field wire connection.

C. Neutral Wire Overlapping Transfer Test

The test of the neutral wire overlapping transfer has been carried out, and the result is shown in Fig. 19. The time that ATS1 is in B-position and ATS2 is in A-position is the overlapping time (T_{overlap}). From the figure, this time is about 40 ms.

Transfer strategy experiments describe the transfer processes which can give a reference to select a suitable strategy according to the customer's demands. Short-circuit experiments show the HATS never operates incorrectly, and this is very useful in actual use. The function neutral wire overlapping transfer guarantees the ground protection of the load during the transfer process.

V. Field Experiments

A. Field Wire Connection

The prototype is installed in a pumping station of Wuhan Iron and Steel Corporation as Fig. 20 shows. Expect that the main water pumps (1#–8#), other loads, such as the vacuum

TABLE II
Field Parameters

Preferred source	10kV/400V 1000kVA transformer 2B
Alternate source	10kV/400V 1000kVA transformer 1B
Power of single pump	155kW
System type	TN-C

pump, and lights (single loads) are also connected to the two 400-V buses. Before the HATS is installed, bus I fetches power from transformer 1B through the circuit breaker 1QF, and bus II gets power from 2B through 2QF. The two bus voltages usually are in phase. The tie breaker 3QF is on the OFF state. When one of the feeders fails, the operator gives the opening signal to the corresponding breaker (1QF or 2QF) manually and then gives the closing signal to 3QF, and then, the bus whose feeder has failed gets power from the other bus. According to the operation records, this manual transfer process takes several seconds, the pumps shake violently, and the lights flash during the process. These phenomena indicate that there are seconds of voltage interruptions and the bus voltage has an unstable time after transfer operation occurred. Now, the HATS is installed before the bus II, as Fig. 20 shows. Therefore, it will take responsibility for that bus. When the preferred feeder (10-kV II) fails, the HATS will transfer bus II to its alternate feeder (10-kV I) automatically. The customer requires that the HATS can minus the shaking of the pumps when transfer operation happens. The main parameters are listed in Table II.

B. Field Experiment Results

Only one of the water pumps was running when the experiments were in progress, and the load current reached 230 A. The preferred source was interrupted by the manual shutdown of the 2QF. The manual mode transfer and the four transfer strategies have been tested. In the manual mode, the operator gives a transfer signal by pushing a button, and then, the controller controls the transfer. The load phase voltages and currents shown in Fig. 21 are measured and recorded by the fault recorder ZH-102 produced by Zhongyuan-Huadian Company, Ltd. The measure point is marked in Fig. 20. After 2QF opens the circuit, the load currents are cut off, but the load voltages (A-phase and C-phase) have only a little change. This phenomenon is caused by the regenerated voltage of the motor. The B-phase voltage decays rapidly because there are some lamp loads that fetch power from the B phase. Transfer times and the peak currents of three phases before and after the transfer are marked in each figure.

Fig. 21(b) looks the same with Fig. 21(c), and this is because the BBM strategy and the natural commutation strategy nearly go in the same way with the preferred source three-phase open circuit. In this application (mainly motor load), Fig. 21 shows that the longer transfer process means a higher transient peak value of the current after the transfer. The transient processes are different according to the different transfer times. The relationship between the multiple of the inrush current and transfer time is shown in Fig. 22.

Fig. 21 shows that the transfer times of all the processes are less than 35 ms; during the experiments, the pumps do

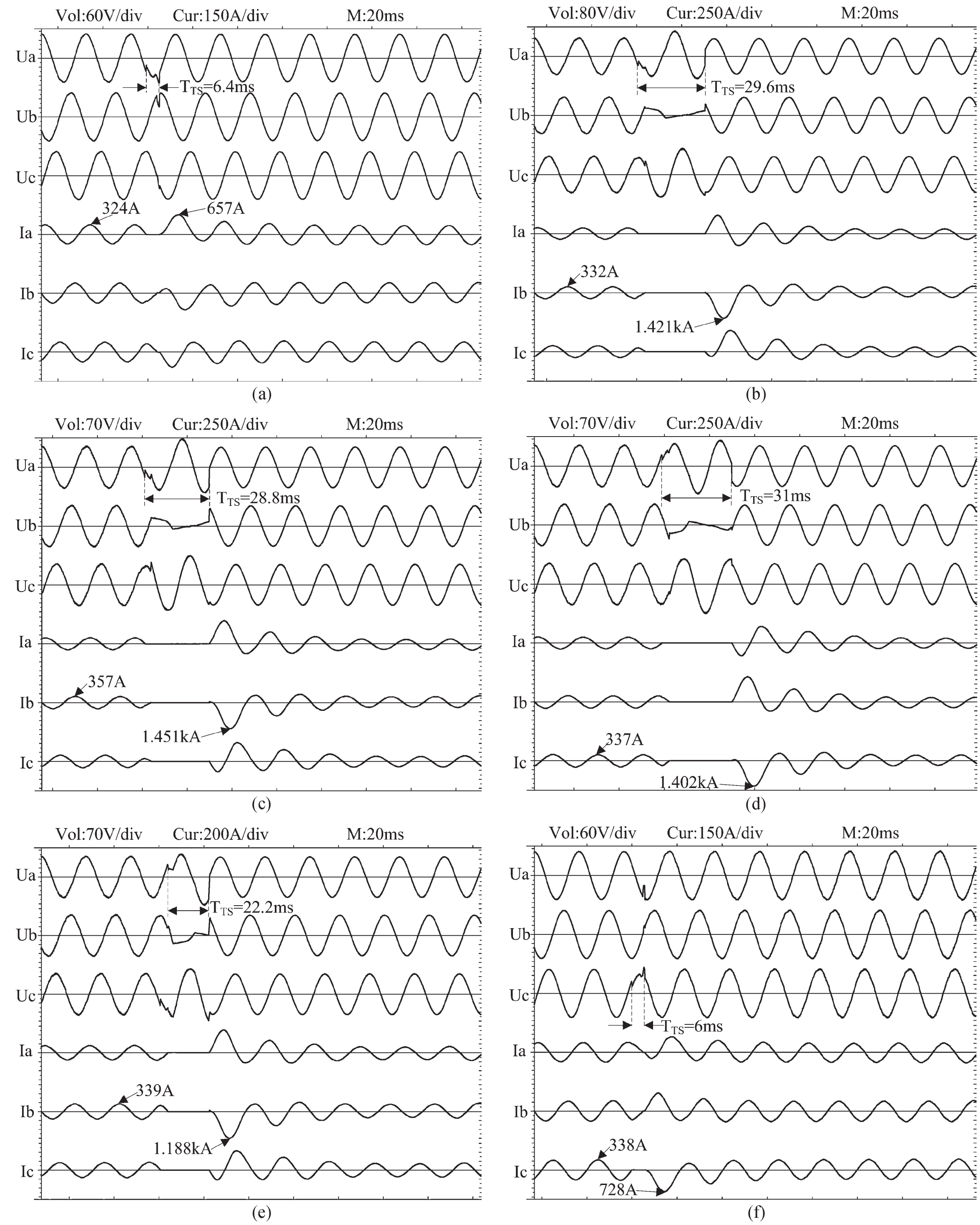

Fig. 21. Load voltage and current waves of the field experiment (recorded by fault recorder). (a) Transfer in the manual mode. (b) Transfer under the BBM strategy. (c) Transfer under the natural commutation strategy. (d) Transfer under the mechanical-switch-breaking-the-circuit strategy. (e) Transfer under the MBB strategy. (f) Return to preferred source in automatic mode.

not shake, and the lights in the same bus do not flash. In fact, due to the inertia of the motor, such interruption does little harm to the pumps. Therefore, all of the four transfer strategies proposed can meet the costumer's requirement. Since the two sources are usually in phase, the MBB strategy is suitable for this application because it has the smallest impact on load.

Field experiments verify that the HATS is functional. In the Wuhan Iron facility, there are many voltage-sensitive loads such as precision instruments, which will be seriously affected by one or more cycles of voltage interruptions, and it demands the neutral wire to never be cut off at any time. The proposed HATS can meet the need and will be used for these critical loads.

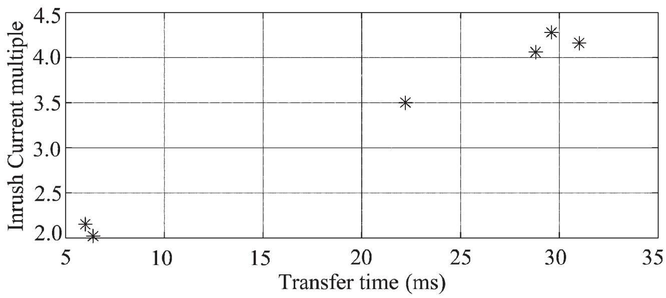

Fig. 22. Relationship between the multiple of the inrush current and the transfer time.

VI. Conclusion

The transfer switch is one of the most cost-effective solutions to the power quality problems. This paper proposed a HATS which has the following features and advantages.

1) Four transfer strategies can be chosen for different applications.
2) It has the function of fault location identification.
3) It has overlapping transfer of the neutral wire.

Operation principles, design details, and experiments are also presented in this paper. Laboratory tests and field experiments show that the HATS is functional and works very well.

References

[1] M. J. Sullivan, T. Vardell, and M. Johnson, "Power interruption costs to industrial and commercial consumers of electricity," *IEEE Trans. Ind. Appl.*, vol. 33, no. 6, pp. 1448–1458, Nov./Dec. 1997.

[2] K. H. Kwan, P. L. So, and Y. C. Chu, "An output regulation-based unified power quality conditioner with Kalman filters," *IEEE Trans. Ind. Electron.*, vol. 59, no. 11, pp. 4248–4262, Nov. 2012.

[3] J. M. Guerrero, P. C. Loh, T.-L. Lee, and M. Chandorkar, "Advanced control architectures for intelligent microgrids—Part II: Power quality, energy storage, and ac/dc microgrids," *IEEE Trans. Ind. Electron.*, vol. 60, no. 4, pp. 1263–1270, Apr. 2013.

[4] F. Gonzalez-Espin, E. Figueres, and G. Garcera, "An adaptive synchronous-reference-frame phase-locked loop for power quality improvement in a polluted utility grid," *IEEE Trans. Ind. Electron.*, vol. 59, no. 6, pp. 2718–2731, Jun. 2012.

[5] M. A. P. De Azpeitia, A. Fernandez, D. G. Lamar, M. Rodriguez, and M. M. Hernando, "Simplified voltage-sag filler for line-interactive uninterruptible power supplies," *IEEE Trans. Ind. Electron.*, vol. 55, no. 8, pp. 3005–3011, Aug. 2008.

[6] D. Mahinda Vilathgamuwa, H. M. Wijekoon, and S. S. Choi, "A novel technique to compensate voltage sags in multiline distribution system—The interline dynamic voltage restorer," *IEEE Trans. Ind. Electron.*, vol. 53, no. 5, pp. 1603–1611, Oct. 2006.

[7] J. A. Munoz, J. R. Espinoza, C. R. Baier, L. A. Moran, E. E. Espinosa, P. E. Melin, and D. G. Sbarbaro, "Design of a discrete-time linear control strategy for a multicell UPQC," *IEEE Trans. Ind. Electron.*, vol. 59, no. 10, pp. 3797–3807, Oct. 2012.

[8] A. Luo, S. Peng, C. Wu, J. Wu, and Z. Shuai, "Power electronic hybrid system for load balancing compensation and frequency-selective harmonic suppression," *IEEE Trans. Ind. Electron.*, vol. 59, no. 2, pp. 723–732, Feb. 2012.

[9] J. D. Barros and J. F. Silva, "Multilevel optimal predictive dynamic voltage restorer," *IEEE Trans. Ind. Electron.*, vol. 57, no. 8, pp. 2747–2760, Aug. 2010.

[10] J. W. Schwartzenberg and R. W. De Doncker, "15 kV medium voltage static transfer switch," in *Conf. Rec. 30th IEEE IAS Annu. Meet.*, Oct. 1995, pp. 2515–2520.

[11] H. Mokhtari, M. R. Iravani, S. B. Dewan, P. Lehn, and J. A. Martinez, "Benchmark systems for digital computer simulation of a static transfer switch," *IEEE Trans. Power Del.*, vol. 16, no. 4, pp. 724–731, Oct. 2001.

[12] M. N. Moschakis and N. D. Hatziargyriou, "A detailed model for a thyristor-based static transfer switch," *IEEE Trans. Power Del.*, vol. 18, no. 4, pp. 1442–1449, Oct. 2003.

[13] H. Ashour, "Automatic transfer switch (ATS) using programmable logic controller (PLC)," in *Proc. IEEE ICM*, Jun. 2004, pp. 531–535.

[14] J. Mazumdar, "Application of transfer switch in mining converters," in *Conf. Rec. 45th IEEE IAS Annu. Meet.*, Oct. 2010, pp. 1–5.

[15] C. Meyer and R. W. De Doncker, "Solid-state circuit breaker based on active thyristor topologies," *IEEE Trans. Power Electron.*, vol. 21, no. 2, pp. 450–458, Mar. 2006.

[16] P.-T. Cheng and Y.-H. Chen, "Design of an impulse commutation bridge for the solid-state transfer switch," *IEEE Trans. Ind. Appl.*, vol. 44, no. 4, pp. 1249–1258, Jul./Aug. 2008.

[17] D. L. Ransom, "Choosing the correct transfer switch," in *Conf. Rec. Annu. IEEE PPIC*, Jun. 2012, pp. 170–175.

[18] H. Mokhtari, S. B. Dewan, and M. Reza Iravani, "Analysis of a static transfer switch with respect to transfer time," *IEEE Trans. Power Del.*, vol. 17, no. 1, pp. 190–199, Jan. 2002.

[19] H. Mokhtari and M. Reza Iravani, "Effect of source phase difference on static transfer switch performance," *IEEE Trans. Power Del.*, vol. 22, no. 2, pp. 1125–1131, Apr. 2007.

[20] H. Yasaman and H. Mokhtari, "Performance evaluation of hybrid transfer switches in grounded and ungrounded medium-voltage electrical systems," in *Proc. CIGRE/IEEE PES Int. Symp. Qual. Secur. Elect. Power Del. Syst.*, Oct. 2003, pp. 91–96.

[21] M. Takeda, H. Yamamoto, T. Aritsuka, I. Kamiyama, and G. F. Reed, "Development of a novel hybrid switch device and application to a solid-state transfer switch," in *Proc. IEEE Power Eng. Soc. Winter Meeting*, Feb. 1999, vol. 2, pp. 1151–1156.

[22] M. Takami, T. Ise, and K. Tsuji, "Studies toward a faster, stabler and lower losses transfer switch," in *Proc. IEEE Power Eng. Soc. Winter Meeting*, Jan. 2000, vol. 4, pp. 2729–2734.

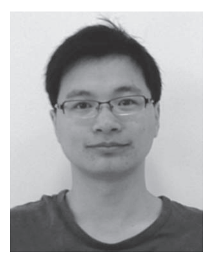

Bing Tian received the B.S. and M.S. degrees from the Department of Electrical Engineering, Huazhong University of Science and Technology, Wuhan, China, in 2009 and 2012, respectively, where he is currently working toward the Ph.D. degree.

His research interest is the application of power electronic technology in power systems.

Chengxiong Mao (M'93–SM'07) received the B.S., M.S., and Ph.D. degrees from the Department of Electrical Engineering, Huazhong University of Science and Technology (HUST), Wuhan, China, in 1984, 1987, and 1991, respectively.

He was a Visiting Scholar at the University of Calgary, Calgary, AB, Canada, from January 1989 to January 1990 and at Queen's University of Belfast, Belfast, U.K., from December 1994 to December 1995. He was conducting research at the Technische Universitaet Berlin, Berlin, Germany, from April 1996 to April 1997 with the support of the Humboldt Foundation. He is currently a Professor with HUST. His fields of interest are power system operation and control, excitation control of synchronous generators, and applications of high-power electronic technology to power systems.

Jiming Lu was born in Jiangsu, China, in 1956. He received the B.S. degree from the Department of Electrical Engineering, Shanghai Jiaotong University, Shanghai, China, and the M.S. degree from the Department of Electrical Engineering, Huazhong University of Science and Technology (HUST), Wuhan, China.

In 1984, he joined the faculty of HUST. He is currently a Professor with the Department of Electrical Engineering, HUST. His research is focused on excitation control based on a microcomputer.

Dan Wang (M'07) received the B.S., M.S., and Ph.D. degrees from the Department of Electrical Engineering, Huazhong University of Science and Technology (HUST), Wuhan, China, in 1999, 2002, and 2006, respectively.

He was a Postdoctoral Researcher, from 2006 to 2008, sponsored by the China Postdoctoral Science Foundation in the Department of Control Science and Engineering, HUST. From 2008 to 2009, he was a Visiting Research Associate in the Department of Electrical and Computer Engineering, Michigan State University, East Lansing, MI, USA. In 2008, he joined HUST, where he is currently an Associate Professor. His research interests include power system operations and control and power conditioning and grid connection of alternative energy sources.

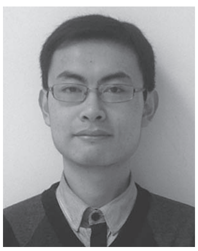

Yu He received the B.S. degree from the Department of Electrical Engineering, Huazhong University of Science and Technology, Wuhan, China, in 2011, where he is currently working toward the Ph.D. degree.

His research interests include applications of power electronics to power systems and excitation control of generators.

Yuping Duan was born in 1964. He received the B.S. degree from the Department of Electrical Engineering, Huazhong University of Science and Technology, Wuhan, China, in 1985.

He is currently a Senior Engineer with Wuhan Iron and Steel (Group) Corporation (WISCO), Wuhan, China, and he engages in the operation and management of distribution networks. His research is focused on grid operation and reactive power optimization.

Jun Qiu was born in 1970. He received the M.S. degree from Wuhan University of Hydraulic and Electrical Engineering, Wuhan, China, in 1992.

He is currently a Senior Engineer with Wuhan Iron and Steel (Group) Corporation (WISCO), Wuhan, and his research interests include grid operation and safety management of electrical systems.